

14 Mar 1991, 10:30 am - 12:30 pm

Earthquake-Induced Settlement in Soft Grounds

K. Yasuhara
Ibaraki University, Japan

T. Konami
Yamaguchi University, Japan

M. Hyodo
Yamaguchi University, Japan

K. Hirao
Nishinippon Institute of Technology, Japan

Follow this and additional works at: <https://scholarsmine.mst.edu/icrageesd>



Part of the [Geotechnical Engineering Commons](#)

Recommended Citation

Yasuhara, K.; Konami, T.; Hyodo, M.; and Hirao, K., "Earthquake-Induced Settlement in Soft Grounds" (1991). *International Conferences on Recent Advances in Geotechnical Earthquake Engineering and Soil Dynamics*. 17.

<https://scholarsmine.mst.edu/icrageesd/02icrageesd/session03/17>



This work is licensed under a [Creative Commons Attribution-Noncommercial-No Derivative Works 4.0 License](#).

This Article - Conference proceedings is brought to you for free and open access by Scholars' Mine. It has been accepted for inclusion in International Conferences on Recent Advances in Geotechnical Earthquake Engineering and Soil Dynamics by an authorized administrator of Scholars' Mine. This work is protected by U. S. Copyright Law. Unauthorized use including reproduction for redistribution requires the permission of the copyright holder. For more information, please contact scholarsmine@mst.edu.



Earthquake-Induced Settlement in Soft Grounds

K. Yasuhara

Department of Civil Engineering, Ibaraki University, Hitachi, Ibaraki, 316, Japan

M. Hyodo

Department of Civil Engineering, Yamaguchi University, Ube, Yamaguchi, 755, Japan

T. Konami

Graduate Student, Department of Civil Engineering, Yamaguchi University, Ube, Yamaguchi, 755, Japan

K. Hirao

Department of Nishinippon Institute of Technology, Kanda, 1633, Fukuoka, 800-03, Japan

SYNOPSIS : Earthquake-induced settlements in clay is derived from both undrained shear deformation and post-earthquake volume change. The former is assumed to be time-independent while the latter must be time-dependent. To determine the characteristics of cyclic-induced settlements, the authors have carried out a family of cyclic triaxial tests followed by drainage on the plastic marine clay. In every test, shear strain and excess pore pressure were measured during undrained stage and volume change was measured during dissipation of excess pore pressure. In the present study, in particular, the results from cyclic triaxial tests were formulated in order to predict the variations of pore pressure with number of load cycles. An excess pore pressure model was used together with the consolidation theory to evaluate the total settlements and their time-dependent variations due to dissipation of cyclic-induced pore pressure. The results of analysis using the proposed method provide a basis for evaluating the post-earthquake settlement in soft grounds.

INTRODUCTION

Cyclic-induced settlements are divided into two categories: residual settlement during undrained cyclic loading and post-cyclic settlement due to dissipation of excess pore pressure generated during cyclic loading. When evaluating the one-dimensional settlement of soft grounds due to horizontal shaking of earthquakes, the latter is considered to be sometimes more predominant than the former. The settlement of this kind in soft grounds was observed in the 1957 Mexico Earthquake and the 1986 Miyagioki Earthquake in Japan, and has been regarded as an important problem from the geotechnical engineering point of view included in earthquakes, although cyclic-induced settlements are not so dramatic compared as the failure during earthquakes.

The present paper describes a simplified and practical method for evaluating this post-earthquake settlement in soft grounds due to dissipation of excess pore pressures generated during earthquakes. The evaluating procedure is based on combination of the results from cyclic triaxial tests with the consolidation theory.

SIMPLIFIED PROCEDURE OF EVALUATING THE EARTHQUAKE-INDUCED SETTLEMENT

As illustrated in Fig. 1, the total settlement of structures founded on clay, S_T , induced by earthquakes consists of the immediate settlement, S_U , during earthquake, and the post-earthquake cyclic settlement, S_{VR} . That is, we have :

$$S_T = S_U + S_{VR} \quad (1)$$

The former occurs under the constant volume condition while the latter accompanies the decrease in soil volumes following the undrained immediate settlement.

In the previous study by the authors (Yasuhara

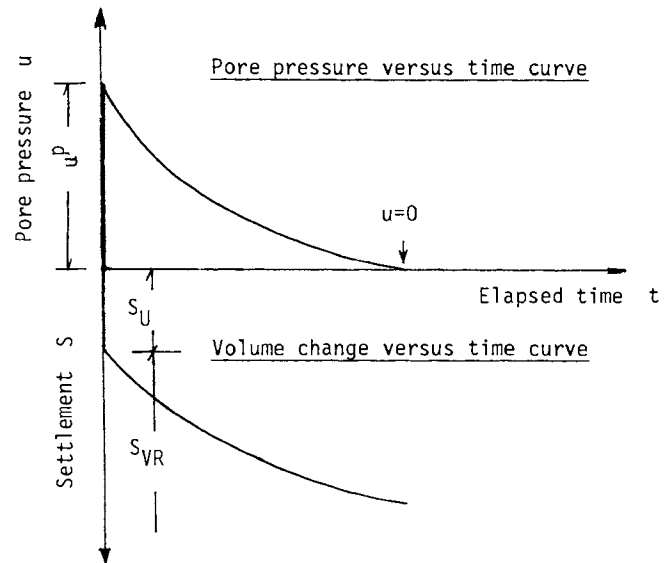


Fig. 1 Schematic illustration for behavior during and after undrained cyclic loading

and Andersen, 1989 : 1990), the post-cyclic volumetric strain, ϵ_{VR} , was primarily governed by the maximum pore pressure, u_f , generated during undrained loading. The magnitude of this volumetric strain was given by :

$$\epsilon_{VR} = \alpha \cdot \frac{C_r}{1 + e_0} \log \left(\frac{1}{1 - u/\sigma'_c} \right) \quad (2)$$

where α : experimental constant, C_r : recompression index, e_0 : void ratio corresponding to the initial vertical stress, σ'_{vc} . Post-earthquake settlements in clay are evaluated using Eq. (2) when the cyclic-induced pore pressure, u , included in Eq. (2) is given by :

$$u = f(\tau_d/\sigma_{vc}, N) \quad (3)$$

where τ_d/σ_{vc} is the cyclic shear stress ratio, N is the number of load cycles. According to the study by Seed, et al. (1971), the cyclic shear stress included in Eq. (3) are estimated by :

$$\frac{\tau_d}{\sigma'_v} = \frac{\alpha_{eg}}{g} \frac{\sigma_v}{\sigma'_v} r_d \quad (4)$$

where α_{eg} is equivalent surface acceleration, σ'_v , σ_v are effective and total vertical stress, $r_d = 1 - 0.015z$ (z : depth of the ground) proposed by Iwasaki et al. (1978).

As the second step, when combining Eq. (3) with the one-dimensional consolidation theory :

$$\frac{\partial u_g}{\partial t} = \left(\frac{k_r}{m_{vr} \gamma_w} \right) \frac{\partial^2 u_g}{\partial z^2} \quad (5)$$

where k_r , m_{vr} are coefficients of permeability and compressibility during recompression, respectively, we can predict the variations of excess pore pressure dissipation and its following recompression volumetric strain with the elapsed time. It is essential in performing the numerical analysis to determine the values of m_{vr} and k_r included in Eq. (5). This can be done by using the results from undrained cyclic triaxial tests followed by drainage. A series of tests can give us information available for formulating both the cyclic-induced excess pore pressure and the post-cyclic recompression volumetric strain characteristics.

CYCLIC TRIAXIAL TESTS

A family of cyclic triaxial tests on the isotropically consolidated marine clay specimens with 5 cm diameter and 10 cm height were carried out to investigate the undrained nature and post-cyclic behavior which should be

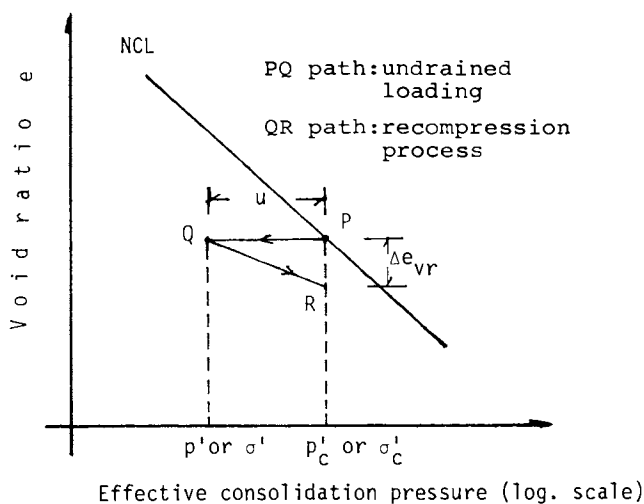


Fig. 2 $e - \log p'$ (or $\log \sigma'_c$) representation for explanation of the post-recompression behavior

utilized for post-earthquake settlement analysis. A cyclic stress, τ_d , given in the form of the stress level, τ_d/σ_{vc} (where $\tau_d = \sigma_d/2$), was applied to a specimen through the stress-controlled conditions with 0.1 Hz. of frequency. The confining pressure in all of the tests was 196 kPa.

After the specimen was subjected to a certain number of load cycles and uniform distribution of excess pore pressures was ensured by leaving the specimen for a few hours under the initial isotropic stress condition, the drainage line was open with measurement of volume changes and their time-dependency during dissipation of excess pore pressure. The duration for measurement of recompression volume change is 4 hr. on average which approximately corresponds to the end of primary consolidation in most of tests. The state path by the $e - \log \sigma'_c$ representation for this kind of tests is demonstrated in Fig. 2.

FORMULATION OF THE RESULTS FROM UNDRAINED CYCLIC TRIAXIAL TESTS

Cyclic pore pressure formulation

Cyclic triaxial testing conditions are outlined in Table 1. Fig. 3 shows a typical result from cyclic triaxial tests on a highly plastic marine clay ($G_s = 2.58$, $w_L = 115\%$, $I_p = 72$). In undrained cyclic triaxial tests on the clay, as are illustrated in Fig. 3, excess pore pressures build up, and cyclic strains increase gradually with increasing the number of load cycles and then a clay specimen leads to failure.

Table 1 Triaxial testing conditions

Test No.	w_i (%)	e_c	q_{cyc}/p_c	N_{max} (cycles)
K-26	65.8	1.687	0.60	6
K-27	66.4	1.691	0.55	12
K-16	66.5	1.690	0.50	11
K-20	66.8	1.724	0.45	24
K-25	65.8	1.683	0.40	543
K-12	64.5	1.660	0.375	1674
D-1	66.6	1.696	0.55	11
D-2	67.8	1.735	0.50	36
D-4	66.5	1.700	0.45	10002
D-5	66.9	0.850	0.40	10000

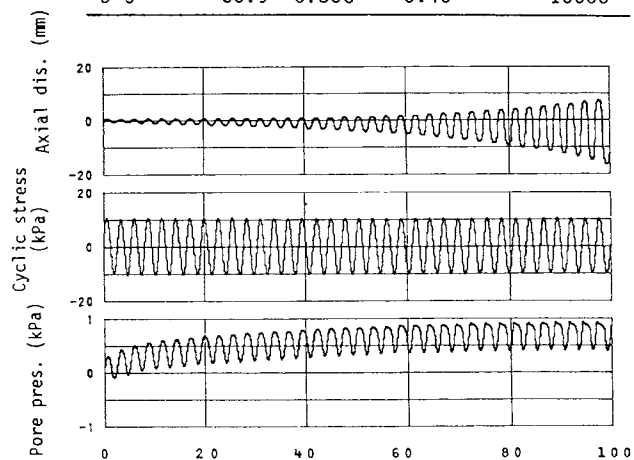


Fig. 3 Typical results from cyclic triaxial test

Fig. 4 illustrates by means of the both logarithmic scales a relation between the cyclic stress ratio, $(q_{cyc}/p'_c)_f$, ($q_{cyc} = \sigma_d$, $p'_c = \sigma'_c$) required for the 5% double amplitude of shear strain and the number of load cycles, N_f . The results in Fig. 4 are then formulated into:

$$R_f = (q_{cy}/p_c)_f = a N_f^b \quad (6)$$

where a and b are experimental constants, equal to 0.624 and -0.071, respectively, for a reconstituted Ariake clay used in the present study.

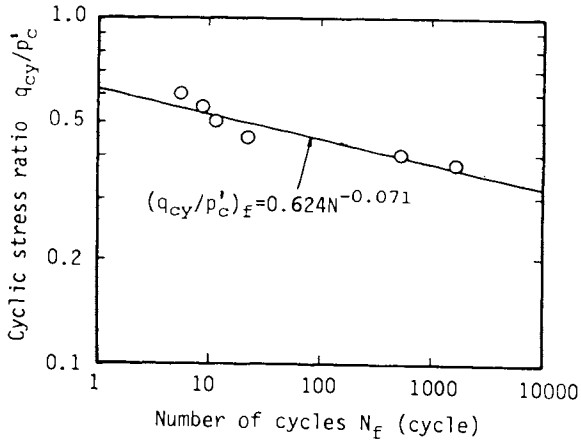


Fig. 4 Cyclic stress ratio versus number of load cycles relation at 5% double amplitude axial strain

By referring to the schematic diagram of p' - q spaces illustrated in Fig. 5, the excess pore

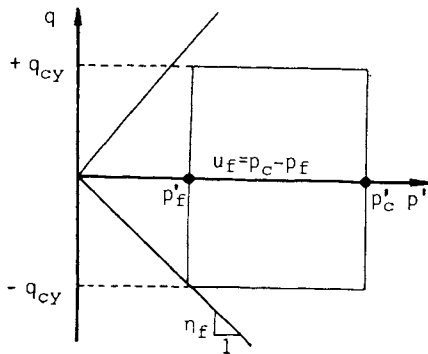


Fig. 5 Definition of the pore pressure at cyclic failure

pressure, u_f , generated at failure in the extension side for a given number of load cycles is written as:

$$u_f = p_c - p_f = q_{cy}/\eta_f \quad (7)$$

where η_f is the effective stress ratio at failure which is defined in the present study as each specimen reaching the 5% double amplitude cyclic shear strain.

Here, by referring Fig. 6 and Fig. 7, we introduce the following new parameters in order to formulate the cyclic-induced pore pressure. The first new parameter is:

$$RR = \frac{R_f(1) - R_f(N)}{R_f(1) - R} \quad (8)$$

where $R_f(1)$ and $R_f(N)$ are cyclic strengths at the 1st and N th number of load cycles given by Eq. (6) and, R is the amplitude of applied cyclic shear stress ratio, respectively. As the second new parameter we define:

$$\eta^* = \frac{\eta - \eta_s}{\eta_f - \eta_s} \quad (9)$$

where η is current effective stress ratio, η_s is effective stress ratio at an intersection of the total stress path ($dq/dp'=3$) with the line of $q = -q_{cyc}$. This parameter, η^* , indicates the relative effective stress ratio between initial and failure at the extension side in p' - q spaces. When plotting the values of both two parameters obtained from cyclic triaxial tests, we have Fig. 8, and resultantly we can assume:

$$\eta^* = \frac{RR}{c_1 - (c_1 - 1)RR} \quad (10)$$

(c_1 : experimental constant)

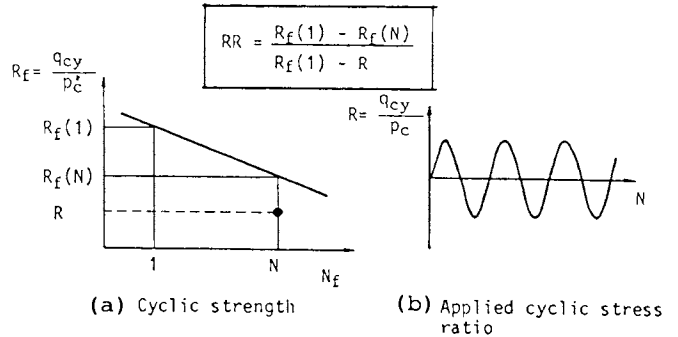


Fig. 6 Definition of the parameter, RR

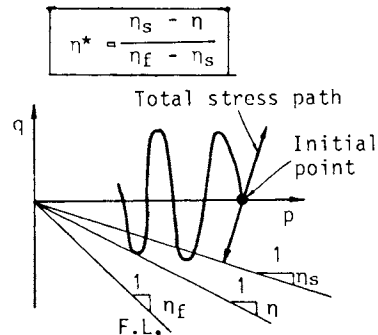


Fig. 7 Definition of the parameter, η^*

The comparison between calculated and observed η^* and RR relations is shown in Fig. 8.

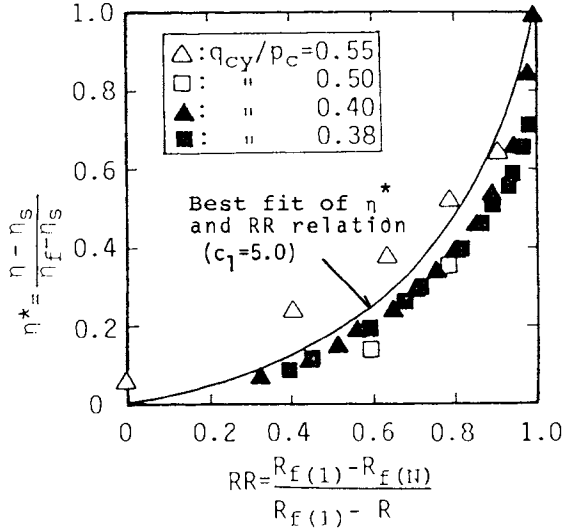


Fig. 8 Correlation of the relative stress ratio to the relative cyclic stress ratio

On the basis of the results from cyclic triaxial tests, we can also obtain a unique relationship between pore pressure ratio, u/u_f and η^* which is shown in Fig. 9. This relation can also be formulated as follows:

$$\frac{u}{u_f} = \frac{\eta^*}{c_2 - (c_2 - 1)\eta^*} \quad (11)$$

where u_f is the ultimate maximum residual pore pressure as was previously shown in Fig. 5. By combining Eq. (8), Eq. (10) and Eq. (11), we have:

$$\frac{u}{u_f} = \frac{R_f(1) - R_f(N)}{c_1 c_2 \{R_f(N) - R\} + \{R_f(1) - R_f(N)\}} \quad (12)$$

where c_1 and c_2 are experimental constants included in Eq. (10) and Eq. (11), respectively.

The good agreement between observed values and calculated values using Eq(12) is proved in Fig. 9. Subsequently, the ratio of residual pore pressure to the initial confining effective stress

$$\frac{u}{\sigma'_c} = \frac{u}{u_f} \cdot \frac{u_f}{\sigma'_c} \quad (13)$$

In order to verify the procedure given by Eq. (13), the calculated excess pore pressures are compared in Fig. 10 with the values measured in cyclic triaxial tests on a reconstitute Ariake clay. The comparison in Fig. 10 shows a fairly good agreement for the variations of build-up excess pore pressure with time during undrained cyclic loading.

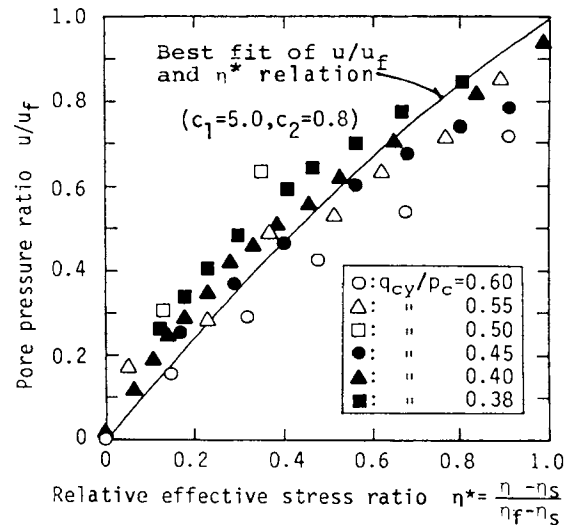


Fig. 9 Relation between cyclic-induced pore pressure ratio and relative effective stress ratio

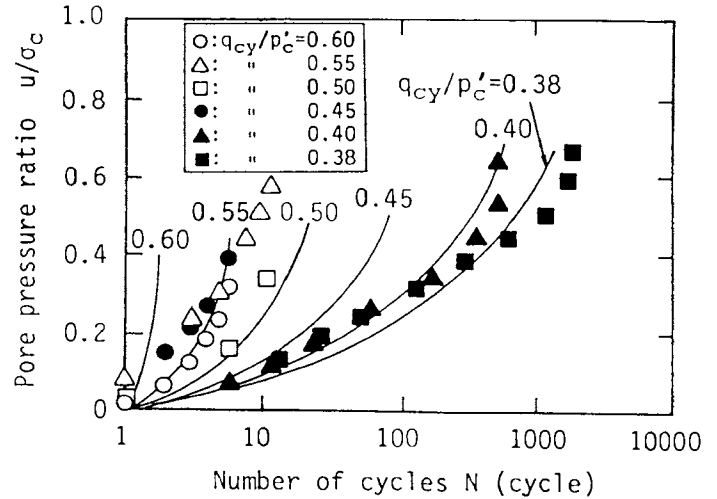


Fig. 10 Comparison between calculated and observed cyclic-induced pore pressures related to number of load cycles

Post-earthquake recompression

After the clay specimen is subjected to a certain number of load cycles under undrained conditions and then was left for a few hours to ensure uniform distribution of excess pore pressures, the drainage line in the triaxial equipment was open with measurement of the dissipating pore pressure and the accompanying volumetric change.

Based on the results from cyclic triaxial tests with drainage and Eq. (2), the coefficient of volume compressibility, m_{vr} , was obtained as follows:

$$m_{vr} = \alpha \frac{C_r}{1 + e_o} \frac{1}{\sigma'_c - u_p} \quad (14)$$

Since the coefficient of reconsolidation, c_{vr} , was determined from the recompression volumetric strain versus elapsed time curves, the coefficient of permeability, k_r , is given by :

$$k_r = c_{vr} \cdot \gamma_w \cdot m_{vr} \quad (15)$$

Thus, the variations of recompression volumetric strain with elapsed time for radial drainage like in the specimen in the triaxial cell can be pursued using the two-dimensional consolidation theory given by :

$$\frac{\partial u}{\partial t} = \frac{k_r}{m_{vr} \gamma_w} \nabla^2 u \quad (16)$$

As the examples the comparison between calculated and observed values of ϵ_{vr} and u^p plotted against elapsed time is shown in Fig. 11.

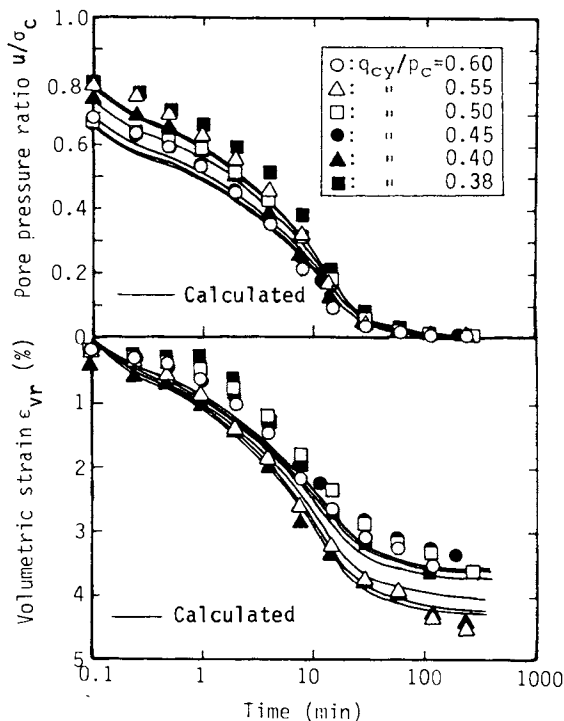


Fig. 11 Variations of post-cyclic pore pressure and volumetric strain with elapsed time

APPLICATION OF SIMPLIFIED PROPOSED METHOD

The model ground consisting of the Ariake clay used in triaxial tests to formulate the cyclic-induced pore pressure behavior was assumed in Fig. 12. The procedure of evaluating the post-earthquake settlement of the model ground in Fig. 12 based on the results from triaxial tests and their formulations is described as follows:

1) The cyclic stress ratio at an arbitrary depth

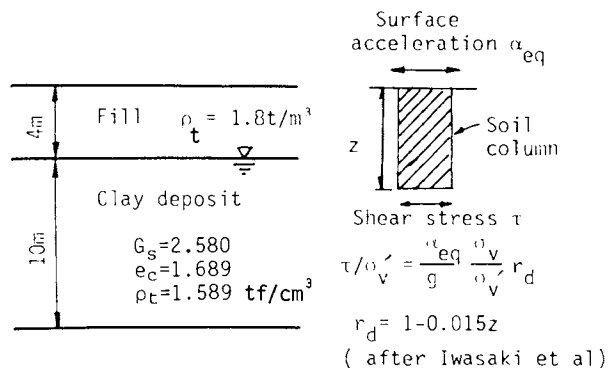


Fig. 12 A model ground for calculation

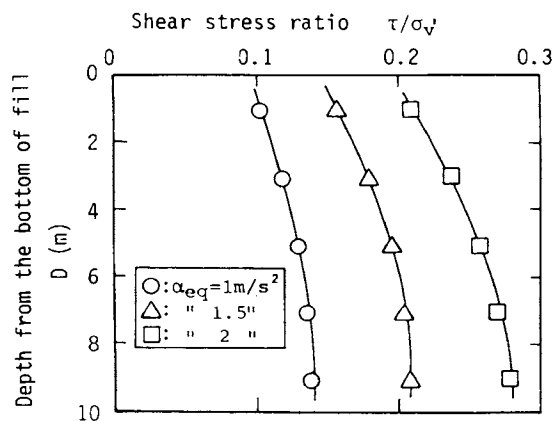


Fig. 13 Variations of shear stress ratio with depth for each surface acceleration

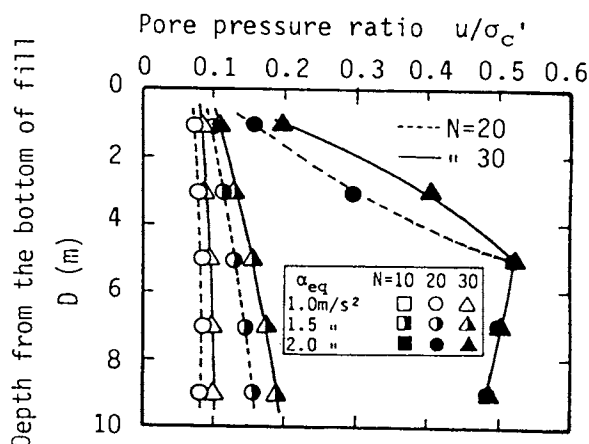


Fig. 14 Variations of pore pressure ratio with depth for respective values of α_{eq} and N

of the ground is determined using Eq. (4). The distributing of the shear stress ratio is shown in Fig. 13, indicating that the cyclic stress ratio increases with the depth of the ground.

2) The amount of cyclic-induced pore pressure shown in Fig. 14 is estimated using the previously described procedure and Eq. (13).

Results of the variations of calculated pore pressure with the depth point out that;

i) In case of $\alpha_{eq} = 1$ and 1.5 m/s^2 (α_{eq} = surface acceleration), the excess pore pressure ratio, u/σ_{vc} , at each number of load cycles ($N=10, 20$ and 30) increases with the depth, as shown in Fig. 14.

ii) In case of $\alpha_{eq} = 2.0 \text{ m/s}^2$, the two lower layers lead to failure (namely, $u/u_f = 1.0$) under $N = 10$ while under $N = 20$ and 30 the three lower layers are failed.

iii) The pore pressure at failure becomes smaller at the lower layer than the upper layer of the ground.

3) Determine the settlements of each layer using (2):

$$\epsilon_{vr} = \frac{u/\sigma_c}{0.412 - 0.291 (u/\sigma_c)} \quad (17)$$

which is formulated from the results in Fig. 15 instead of Eq. (2) because the correct value of C_r included in Eq. (2) is not available at the present time for the clay used in the current study.

4) Then sum them up as the total settlement due to dissipation of earthquake-induced pore pressure. The results in the present study are shown in Fig. 16.

CONCLUSIONS

1) Interpretation of the mechanism of earthquake-induced settlements in clay was described and a simplified procedure was proposed for predicting the post-earthquake settlements of clay grounds.

2) The important step included in the proposed method is to model the cyclic-induced pore pressure in clay. For this purpose the results from cyclic triaxial tests on a reconstituted soft clay were formulated to be combined with the consolidation theory.

3) A case study for the post-earthquake settlement of the soft clay ground indicates that the post-earthquake settlement increases with increasing the surface acceleration of the soft ground.

REFERENCES

Hyodo, M., K. Yasuhara and H. Murata (1988), Earthquake induced settlements in clays, Proc. 9th World Conf. Earthquake Eng., Vol. 1. III, pp. III-89 - III-94.

Hyodo, M., H. Murata, N. Yasufuku and T. Fujii (1989), Undrained cyclic shear strength and deformation of sands subjected to initial static shear stress, Proc. 4th Intn'l. Conf. Earthquake Eng., Mexico City, Mexico, pp. 81 - 103.

Iwasaki, T., F. Tatsuoka, K. Tokida and S. Yasuda, A practical method for assessing soil liquefaction potential based on case studies at various sites in Japan, Proc. 5th Earthquake Eng., Symp., pp. 641 - 648.

Yasuhara, K. and K. H. Andersen (1989), Post-cyclic recompression in clay, Proc. 4th Intn'l. Conf. Soil Dynamics and Earthquake Eng., Vol. 1, pp. 159 - 167.

Yasuhara, K. and K. H. Andersen (1990), Discussion to "Study on the settlement of saturated clay layer induced by cyclic shear" by Ohara, S. and H. Matsuda (Soils and Foundations, Vol. 28, No. 3, pp. 103 - 113), Soils and Foundations, Vol. 30, No. 2, pp. 139 - 141.

Seed, H. B. and Idriss, I. M. (1971), Simplified procedure for evaluating soil liquefaction, Proc. ASCE, Vol. 97, No. SM, pp. 1249 - 1273.

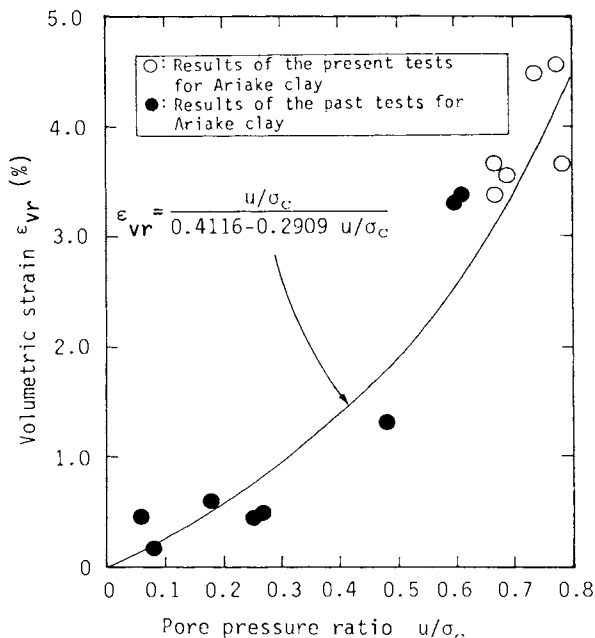


Fig. 15 Post-cyclic recompression volumetric strain versus pore pressure ratio from cyclic triaxial tests

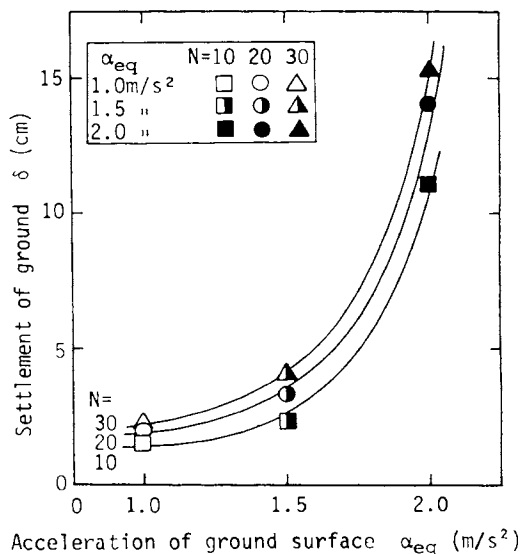


Fig. 16 Settlement of the model ground